Two Crystalline Forms of Low-Spin [Fe(TMP)(5-MeHIm)$_2$]ClO$_4$. Relative Parallel and Perpendicular Axial Ligand Orientations

Orde Q. Munro,[*,†,‡] **Judith A. Serth-Guzzo,**[†] **Ilona Turowska-Tyrk,**[†] **K. Mohanrao,**[†]
Tatjana Kh. Shokhireva,[§] **F. Ann Walker,**[*,§] **Peter G. Debrunner,**[*,⊥] **and**
W. Robert Scheidt[*,†]

*Contribution from the Department of Chemistry and Biochemistry, University of Notre Dame,
Notre Dame, Indiana 46556, Department of Chemistry, University of Arizona, Tucson, Arizona 85721,
Department of Physics, University of Illinois, Urbana, Illinois 61801, and Department of Chemistry,
University of Natal, Private Bag X01, Scottsville 3209, South Africa*

Received May 10, 1999

Abstract: The preparation and characterization of two crystalline forms of [Fe(TMP)(5-MeHIm)$_2$]ClO$_4$ with distinctly different molecular structures are reported. Crystal structure analysis shows that *paral*-[Fe(TMP)-(5-MeHIm)$_2$]ClO$_4$ has the axial imidazole ligands arranged in a relative parallel orientation (over a slightly S_4-ruffled porphyrin core) and *perp*-[Fe(TMP)(5-MeHIm)$_2$]ClO$_4$ has the axial imidazole ligands arranged in a relative perpendicular orientation (over a considerably S_4-ruffled porphyrin core). The two species have different Mössbauer and solid-state EPR spectra. The small quadrupole splitting ($\Delta E_q = 1.78(1)$ mm/s, 120 K) and a single observable EPR g_{max} value (3.43 at 4.2 K) for *perp*-[Fe(TMP)(5-MeHIm)$_2$]ClO$_4$ are indicative of the relative perpendicular arrangement of the axial ligands. The larger quadrupole splitting ($\Delta E_q = 2.557(3)$ mm/s, 120 K) and rhombic g-tensor ($g_1 = 2.69$, $g_2 = 2.34-2.43$, and $g_3 = 1.75$) in the solid state and in frozen DMF−acetonitrile 3:1 ($g_1 = 2.64$, $g_2 = 2.30$, and $g_3 = 1.80$) at 4.2 K for *paral*-[Fe(TMP)(5-MeHIm)$_2$]ClO$_4$ are indicative of a relative parallel axial ligand orientation. The actual axial ligand dihedral angles are $\Delta\phi = 76°$ and $\Delta\phi = 26$ or $30°$ for *perp*- and *paral*-[Fe(TMP)(5-MeHIm)$_2$]ClO$_4$, respectively, and thus the dihedral angle at which the EPR spectral type changes from large g_{max} to rhombic must be $30 < \Delta\phi < 76°$. Because the porphyrin and axial ligands are similar for both crystalline forms of [Fe(TMP)(5-MeHIm)$_2$]ClO$_4$, a more direct correlation between molecular and electronic structure has been established. Molecular mechanics calculations indicate that nonbonded interactions between the axial ligands and *meso*-mesityl groups of [Fe-(TMP)(5-MeHIm)$_2$]$^+$ destabilize a relative parallel orientation for the axial ligands, yet the parallel orientation is observed in all frozen solution samples as confirmed by EPR investigations. This is believed to be due to the competing stabilization of the electronic state of the rhombically distorted parallel complex with an energy stabilization of 2.8−3.7 kcal/mol, as compared to the energy destabilization of 2.6 kcal/mol obtained from MM calculations.

Introduction

Currently there are three X-ray structures of tetraheme cytochromes with bis-histidine coordination of the heme iron (the cytochromes c_3 from the sulfate reducing bacteria *Desulfovibrio vulgaris*,[1] *Desulfovibrio desulfuricans*,[2] and *Desulfomicrobium baculatum*[3]) which clearly show unique relative orientations for the pair of axial histidines coordinated to each heme group. In cytochrome c_3 from *D. vulgaris*, for example, three of the four heme groups have relative parallel histidine orientations, while the fourth has a more staggered conformation in which the dihedral angle between the histidine planes is 64° and therefore closer to a relative perpendicular arrangement.[1]

The pair of axial histidines of bovine cytochrome b_5, a monoheme protein, also show a relative near-parallel orientation.[4] In both the cytochromes c_3 and cytochrome b_5, the exact relative orientation(s) of the histidine ligands (and indeed the orientations of the ligand planes relative to the Fe−N$_p$ bonds[5] within the heme group) appear to be important in fine-tuning the heme redox potential. For example, EPR and redox measurements on cytochrome c_3 isolated from several species of sulfate reducing bacteria indicate that each heme iron has a unique electronic structure characterized by well-resolved *g*-

* Authors to whom correspondence should be sent.
† University of Notre Dame.
‡ University of Natal.
§ University of Arizona.
⊥ University of Illinois.

(1) Higuchi, Y.; Kusunoki, M.; Matsuura, Y.; Yasuoka, N.; Kakudo, M. *J. Mol. Biol.* **1984**, *172*, 109−139.
(2) Pierrot, M.; Haser, R.; Frey, M.; Payan, F.; Astier, J. P. *J. Biol. Chem.* **1982**, *23*, 14341−14348.
(3) Czjzek, M.; Guerlesquin, F.; Bruschi, M.; Haser, R. *Structure*, **1996**, *4*, 395−404.

(4) Mathews, F. S.; Czerwinski, E. W.; Argos, P. In *The Porphyrins*; Dolphin, D., Ed.; Academic: New York, 1979; Vol. 7, pp 108−148.
(5) Abbreviations used: BzHIm, benzimidazole; 4-CNPy, 4-cyanopyridine; |C$_m$|, mean absolute displacement of the meso carbons from the porphyrin mean plane; 1,2-Me$_2$Im, 1,2-dimethylimidazole; HIm; imidazole; L, ligand in general; K222, potassium 4,7,13,16,21,24-hexaoxa-1,10-diazabicyclo[8.8.8]hexacosane; 2-MeHIm, 2-methylimidazole; 4(5)-MeHIm, 4(5)-methylimidazole; 1-MeIm, 1-methylimidazole; MM, molecular mechanics; *c*-MU, *cis*-methyl urocanate; N$_{ax}$, axial nitrogen donor; N$_p$, porphinato nitrogen; 4-NMe$_2$Py, 4-*N*,*N*-dimethylpyridine; OEP, 2,3,7,8,-12,13,17,18-octaethylporphyrin dianion; Proto IX, trianion protoporphyrin IX.; T-2,6-Cl$_2$PP, 5,10,15,20-tetra(2,6-dichlorophenyl)porphyrin dianion; TMP, 5,10,15,20-tetramesitylporphyrin dianion; TPP, 5,10,15,20-tetraphenylporphyrin dianion; *t*-MU, *trans*-methyl urocanate; 1-VinIm, 1-vinylimidazole.

values and a discrete redox potential.[6-9] We (and others[10,11]) have shown that the relative orientations of the axial ligands in synthetic low-spin bis-imidazole and bis-pyridine iron(III) porphyrins directly affect the relative energies of the d$_\pi$ orbitals, particularly the half-filled d$_{yz}$ orbital,[12] and thus the type of low-spin EPR spectrum observed.[13,14] Specifically, a relative parallel axial ligand orientation leads to a normal rhombic low-spin **g** tensor with a low-field g_{max} value ≤ 3.0,[15-17] while a relative perpendicular axial ligand orientation leads to near-degeneracy of the d$_{xz}$ and d$_{yz}$ orbitals[10,13] and an EPR spectrum in which the sole observable signal below $\sim$20 K has a g_{max} value >3.2.[15,18,19] This so-called "large g_{max}" value, furthermore, varies with the basicity of the perpendicularly aligned axial ligands.[19]

The crystal structures of the cytochromes c_3,[1-3] cytochrome b_5,[4] and other heme proteins with a single histidine residue coordinated to the heme iron[20-30] reveal that the orientations of the axial ligands are probably controlled by a combination of three factors: (i) covalent attachment of the imidazole group to the protein backbone, (ii) hydrogen bonding between the imidazole N−H proton and H-bond acceptors, most commonly carbonyl groups of the protein backbone,[31] and (iii) nonbonded interactions both with the porphyrin ring and with amino acid

residues within the heme binding pocket.[32] In simple *low-spin* bis-imidazole and bis-pyridine iron(III) porphyrins, axial ligand orientation also appears to hinge on several factors. For *meso*-tetraaryl porphyrins with sterically bulky imidazoles and pyridines, complexes of the type [Fe(TPP)L$_2$]$^+$ and [Fe(TMP)L$_2$]$^+$ show strong S_4-ruffling of the porphyrin core and a relative perpendicular orientation for the axial ligands. From the crystal structures of several of these complexes,[15,18,19,33] and MM-calculated potential surfaces for [Fe(TMP)(1,2-MeIm)$_2$]$^+$ and related species,[34] we have shown that this type of conformation best minimizes unfavorable nonbonded interactions between the axial ligands and the *meso*-aryl substituents. We have also found that strong π-acceptor, weak σ-donor ligands such as 4-cyanopyridine, for example in [Fe(TPP)(4-CNPy)$_2$]ClO$_4$,[35] favor an unusual iron(III) electronic ground state (d$_{yz}$,d$_{xz}$)^4(d$_{xy}$)^1 which, through enhanced d$_\pi$-porphyrin π-backbonding, leads to S_4-ruffling of the porphyrin core and a relative perpendicular orientation for the axial ligands.[36] Finally, in low-spin iron(III) complexes where the steric bulk of the axial and porphyrin ligands is not overly large, relative parallel imidazole and high-basicity pyridine orientations are observed along with near-planar porphyrin core conformations. A relative parallel axial ligand orientation appears favored in these systems as a result of the geometry of the imidazole pπ−metal pπ interaction,[12] as well as the Jahn−Teller stabilization derived from parallel orientations. Structurally characterized examples of bis-imidazole and bis-pyridine complexes with relative parallel axial ligand orientations include [Fe(TMP)(1-MeIm)$_2$]ClO$_4$,[15] [Fe-(TPP)(1-MeIm)$_2$]ClO$_4$,[17] [Fe(TPP)(HIm)$_2$]Cl,[16] [Fe(TPP)(c-MU)$_2$]SbF$_6$,[37] [Fe(TPP)(t-MU)$_2$]SbF$_6$,[37] and [Fe(OEP)(4-NMe$_2$-Py)$_2$]ClO$_4$.[15]

Although the relative orientations of axial imidazoles and pyridines in low-spin iron(III) porphyrins clearly affect the electronic structure of the metal and thus the type of EPR, Mössbauer, and NMR[19,38,39] spectra of these systems, the evidence to date has largely been gathered from studies on complexes with a variety of axial and porphyrin ligands. In this paper we describe the synthesis and characterization of two novel crystalline forms of [Fe(TMP)(5-MeHIm)$_2$]ClO$_4$ in which the axial ligands adopt relative parallel and perpendicular orientations, respectively. We have labeled these two crystalline forms *paral*-[Fe(TMP)(5-MeHIm)$_2$]ClO$_4$ and *perp*-[Fe(TMP)-(5-MeHIm)$_2$]ClO$_4$ to distinguish their near-parallel and near-perpendicular axial ligand arrangements, respectively. Interestingly, these two forms reduce the dihedral angle necessary to

(6) Gayda, J.-P.; Bertrand, P.; More, C.; Guerlesquin, F.; Bruschi, M. *Biochim. Biophys. Acta* **1985**, *829*, 262−267.

(7) Gayda, J.-P.; Benosman, H.; Bertrand, P.; More, C.; Asso, M. *Eur. J. Biochem.* **1988**, *177*, 199−206.

(8) Benosman, H.; Asso, M.; Bertrand, P.; Yagi, T.; Gayda, J.-P. *Eur. J. Biochem.* **1989**, *182*, 51−55.

(9) Moura, I.; Teixeira, M.; Huynh, B. H.; LeGall, J.; Moura, J. J. G. *Eur. J. Biochem.* **1988**, *176*, 365−369.

(10) Inniss, D.; Soltis, S. M.; Strouse, C. E. *J. Am. Chem. Soc.* **1988**, *110*, 5644−5650.

(11) Soltis, S. M.; Strouse, C. E. *J. Am. Chem. Soc.* **1988**, *110*, 2824−2829.

(12) Scheidt, W. R.; Chipman, D. M. *J. Am. Chem. Soc.* **1986**, *108*, 1163−1169.

(13) Walker, F. A.; Huynh, B. H.; Scheidt, W. R.; Osvath, S. R. *J. Am. Chem. Soc.* **1986**, *108*, 5288−5297.

(14) Walker, F. A.; Reis, D.; Balke, V. L. *J. Am. Chem. Soc.* **1984**, *106*, 6888−6898.

(15) Safo, M. K.; Gupta, G. P.; Walker, F. A.; Scheidt, W. R. *J. Am. Chem. Soc.* **1991**, *113*, 5497−5510.

(16) Scheidt, W. R.; Osvath, S. R.; Lee, Y. J. *J. Am. Chem. Soc.* **1987**, *109*, 1958−1963.

(17) Higgins, T.; Safo, M. K.; Scheidt, W. R. *Inorg. Chim. Acta* **1990**, *178*, 261−267.

(18) Scheidt, W. R.; Kirner, J. F.; Hoard, J. L.; Reed, C. A. *J. Am. Chem. Soc.* **1987**, *109*, 1963−1968.

(19) Safo, M. K.; Gupta, G. P.; Walker, F. A.; Watson, C. T.; Simonis, U.; Scheidt, W. R. *J. Am. Chem. Soc.* **1992**, *114*, 7066−7075.

(20) Takano, T. *J. Mol. Biol.* **1977**, *110*, 537−568.

(21) Bolognesi, M.; Onesti, S.; Gatti, G.; Coda, A.; Ascenzi, P.; Brunori, M. *J. Mol. Biol.* **1989**, *205*, 529−544.

(22) Fermi, G.; Perutz, M. F.; Shaanan, B.; Fourme, R. *J. Mol. Biol.* **1984**, *175*, 159−174.

(23) Poulos, T. L.; Freer, S. T.; Alden, R. A.; Edwards, S. L.; Skogland, U.; Takio, K.; Eriksson, B.; Xuong, N.; Yonetani, T.; Kraut, J. *J. Biol. Chem.* **1980**, *255*, 575−580.

(24) Edwards, S. L.; Poulos, T. L. *J. Biol. Chem.* **1990**, *265*, 2588−2595.

(25) Weber, P. C.; Howard, A.; Xuong, N. H.; Salemme, F. R. *J. Mol. Biol.* **1981**, *153*, 399−424.

(26) Finzel, B. C.; Weber, P. C.; Hardman, K. D.; Salemme, F. R. *J. Mol. Biol.* **1985**, *186*, 627−643.

(27) Ochi, H. O.; Hata, Y.; Tanaka, N.; Kakudo, M.; Sakurai, T.; Aihara, S.; Morita, Y. *J. Mol. Biol.* **1983**, *166*, 407−418.

(28) (a) Takano, T.; Dickerson, R. E. *J. Mol. Biol.* **1981**, *153*, 79−94. (b) Takano, T.; Dickerson, R. E. *J. Mol. Biol.* **1981**, *153*, 95−115.

(29) Louie, G. V.; Brayer, G. D. *J. Mol. Biol.* **1990**, *214*, 527−555.

(30) Bushnell, G. W.; Louie, G. V.; Brayer, G. D. *J. Mol. Biol.* **1990**, *214*, 585−595.

(31) Histidine N−H groups are H-bonded to carbonyl oxygens in the following hemoproteins: human deoxyHb, α-chain (His-87···Leu-83); human deoxyHb, β-chain (His-92···Leu-88);[22] sperm whale myoglobin (His-92···Leu-89);[20] *Aplysia* Mb (His-95···Phe-93);[21] and horse, yeast, rice, and tuna cytochrome *c* (His-18···Pro-30).[27-30]

(32) Shelnutt, J. A.; Song, X. Z.; Ma, J. G.; Jia, S. L.; Jentzen, W.; Medforth, C. J. *Chem. Soc. Rev.* **1998**, *27*, 31−41.

(33) Hatano, K.; Safo, M. K.; Walker, F. A.; Scheidt, W. R. *Inorg. Chem.* **1991**, *30*, 1643−1650.

(34) Munro, O. Q.; Marques, H. M.; Debrunner, P. G.; Mohanrao, K.; Scheidt, W. R. *J. Am. Chem. Soc.* **1995**, *117*, 935−954.

(35) Safo, M. K.; Walker, F. A.; Raitsimring, A. M.; Walters, W. P.; Dolata, D. P.; Debrunner, P. G.; Scheidt, W. R. *J. Am. Chem. Soc.* **1994**, *116*, 7760−7770.

(36) We have confirmed this mechanism of S_4-ruffling in low-spin ferric porphyrins with strong π-accepting isocyanide ligands in the ruffled complexes [Fe(TPP)(t-BuNC)$_2$]ClO$_4$ and [Fe(OEP)(t-BuNC)$_2$]ClO$_4$: Walker, F. A.; Nasri, H.; Turowska-Tyrk, I.; Mohanrao, K.; Watson, C. T.; Shokhirev, N. V.; Debrunner, P. G.; Scheidt, W. R. *J. Am. Chem. Soc.* **1996**, *118*, 12109−12118.

(37) Quinn, R.; Valentine, J. S.; Byrn, M. P.; Strouse, C. E. *J. Am. Chem. Soc.* **1987**, *109*, 3301−3308.

(38) (a) Walker, F. A.; Simonis, U. *J. Am. Chem. Soc.* **1991**, *113*, 8652−8657. (b) Shokhirev, N. V.; Shokhireva, T. Kh.; Polam, J. R.; Watson, C. T.; Raffii, K.; Simonis, U.; Walker, F. A. *J. Phys. Chem. A* **1997**, *101*, 2778−2786. (c) Momot, K. I.; Walker, F. A. *J. Phys. Chem. A* **1997**, *101*, 92787−2795; (d) Momot, K. I.; Walker, F. A. *J. Phys. Chem. A* **1998**, *102*, 10682−10688.

(39) Nakamura, M.; Tajima, K.; Tada, K.; Ishizu, K.; Nakamura, N. *Inorg. Chim. Acta* **1994**, *224*, 113−124.

produce the large g_{max} signal and increase that necessary to retain the normal rhombic EPR signal to a difference of 46°, rather than the 90° implied by the terms "parallel" and "perpendicular". The two crystalline forms of [Fe(TMP)(5-MeHIm)$_2$]ClO$_4$ have been prepared by two different synthetic routes; that for *perp*-[Fe(TMP)(5-MeHIm)$_2$]ClO$_4$ is somewhat unusual, but was discovered in our efforts to synthesize the mixed-ligand derivative [Fe(TMP)(4-CNPy)(5-MeHIm)]ClO$_4$. Importantly, this unusual preparation has been reproduced by three of us independently (more than once) and leads to the same crystal polymorph. To our knowledge, this appears to be the first example of two different conformations of the same low-spin iron(III) porphyrin with identical axial ligands.

Experimental Section

General Information. All reactions were performed under an argon atmosphere with Schlenk-ware and cannula techniques. All solvents were distilled under argon prior to use. Chloroform and hexane were distilled from CaH$_2$ and sodium/benzophenone, respectively. 4(5)-Methylimidazole and 4-cyanopyridine were recrystallized from diethyl ether. *meso*-Tetramesitylporphyrin was prepared by a modified version of the procedure published by Lindsey et al.[40] and iron was inserted into H$_2$TMP by standard techniques.[41] [Fe(TMP)OClO$_3$] was prepared as previously described.[15] *Caution!* These perchlorate salts can detonate spontaneously and should be handled only in small quantities; other safety precautions are also warranted. UV−vis spectra were recorded on a Perkin-Elmer Lambda 6 spectrophotometer. Mössbauer measurements were performed at 120 K on a constant acceleration Mössbauer spectrometer on ground single-crystal samples prepared as Apiezon L grease mulls, as previously described.[34] The spectra were least-squares fitted with Lorentzian line shapes. Isomer shifts are quoted relative to iron metal at 300 K. The EPR spectra were obtained on polycrystalline samples at 4.2 K with a Bruker ESP-300E EPR spectrometer operating at X-band and equipped with an Oxford helium cryostat. Glassy EPR samples with varying ratios of 5-MeHIm:Fe were prepared in DMF−acetonitrile 3:1.

Synthesis of *paral*-[Fe(TMP)(5-MeHIm)$_2$]ClO$_4$. [Fe(TMP)OClO$_3$] (210 mg, 0.224 mmol) and 4(5)-MeHIm (210 mg, 2.56 mmol) were placed in a 25-mL Schlenk flask. Chloroform (∼14 mL) was added and the solution was stirred for 10 min. The reaction mixture was transferred to eight 15 × 1.5 cm test tubes and layered with 15 mL of hexane. X-ray quality crystals formed after 4 days. Bulk samples were obtained by selecting the large octagonal plate crystals obtained in the procedure. UV−vis (CHCl$_3$) λ_{max}: 417 (Soret), 552, 580 nm.

Synthesis of *perp*-[Fe(TMP)(5-MeHIm)$_2$]ClO$_4$. Two slightly different procedures were used for this compound. Method A: In each of four 15 × 1.5 cm test tubes were placed [Fe(TMP)OClO$_3$] (15 mg, 0.016 mmol), 4-CNPy (17 mg, 0.163 mmol), and 4(5)-MeHIm (1.5 mg, 0.018 mmol). Each test tube was evacuated and backfilled with argon, and 2 mL of chloroform was added. The solution was then stirred for a few minutes and layered with hexane. After 3 days, X-ray quality crystals were harvested, washed three times with hexane, and dried. These crystals were square plates which were separated from other solid material by hand selection for both bulk samples and X-ray analysis. Method B: [Fe(TMP)OClO$_3$] (75 mg, 0.080 mmol) and 4-CNPy (84 mg, 0.806 mmol) were placed in a 25-mL Schlenk flask. Chloroform (∼5.4 mL) was added and the solution was stirred for 20 min. The UV−vis (CHCl$_3$) spectrum (412, 535, 572 nm) is that of [Fe(TMP)-(4-CNPy)$_2$]ClO$_4$.[15] A chloroform solution of 4(5)-MeHIm (0.080 mmol) was added to the solution with a syringe and stirred for an additional 20 min. A new UV−vis spectrum results (CHCl$_3$): λ_{max} 418 (Soret), 547, 577 nm. The reaction mixture was transferred to four 15 × 1.5 cm test tubes and layered with 15 mL of hexane. X-ray quality crystals formed after 4 days.

Table 1. Crystallographic Details for *paral*- and *perp*-[Fe(TMP)(5-MeHIm)$_2$]ClO$_4$

molecule	*paral*-[Fe(TMP)(5-MeHIm)$_2$]ClO$_4$	*perp*-[Fe(TMP)(5-MeHIm)$_2$]ClO$_4$
formula	FeC$_{70}$H$_{73}$ClN$_{11}$O$_4$	FeC$_{65.2}$H$_{66}$Cl$_{4.6}$N$_8$O$_{4.4}$
formula wt	1223.72	1249.75
solvent/asym unit	3[4(5)-MeHIm]	1.2CHCl$_3$·0.4H$_2$O
a, Å	16.536(6)	15.63(2)
b, Å	19.462(7)	20.96(3)
c, Å	20.127(2)	19.78(3)
β, deg	100.952(15)	99.88(3)
V, Å^3	6359(6)	6434(20)
space group	$P2_1$	$P2_1/n$
Z	4	4
D_c, g/cm^3	1.267	1.382
μ, mm^{-1}	0.330	0.540
λ, Å		0.71073
T, K		127
final R indices^a [$I > 1.5\sigma(I)$]	$R_1 = 0.072$; $R_2 = 0.083$	$R_1 = 0.082$; $R_2 = 0.0890$

^{a} $R_1 = \sum||F_o| - |F_c||/\sum|F_o|$ and $R_2 = [\sum w(|F_o| - |F_c|)^2/\sum w(F_o)^2]^{1/2}$.

X-ray Structure Determinations. The two different black, crystalline forms of [Fe(TMP)(5-MeHIm)$_2$]ClO$_4$ were examined with graphite-monochromated Mo Kα radiation on an Enraf-Nonius FAST area detector diffractometer at 127 K. Unit cell determination and data collection procedures with the area detector have been described previously.[42] A summary of cell constants and refinement results is given in Table 1; complete details are given in Table S1. Slight variations in data collection instrument settings were used owing to differing crystal quality. Data sets were corrected for Lorentz−polarization and absorption effects. The structures were solved by Patterson methods with the SHELXS-86 program.[43] In the *perp*-[Fe-(TMP)(5-MeHIm)$_2$]ClO$_4$ structure there is one independent [Fe(TMP)-(5-MeHIm)$_2$]ClO$_4$ per asymmetric unit, but in the *paral*-[Fe(TMP)(5-MeHIm)$_2$]ClO$_4$ structure there are two such independent moieties in the asymmetric unit. The solvent content of the two crystalline forms was determined during the course of structure solution and refinement. For *perp*-[Fe(TMP)(5-MeHIm)$_2$]ClO$_4$, there is one ordered chloroform molecule and a partially occupied chloroform molecule that is disordered around the inversion center at 1/2, 0, 1/2. There were, in addition, two extra peaks that were refined as partial water molecules. The final model thus had a solvent region divided between two asymmetric units that was occupied either by a CHCl$_3$ (40%) or two water molecules (40%). In *paral*-[Fe(TMP)(5-MeHIm)$_2$]ClO$_4$, there are three imidazole molecules in the asymmetric unit that form a hydrogen bond network with the perchlorate ions and the coordinated imidazoles.

Least-squares refinement of the structural model for both crystals was carried to convergence with anisotropic temperature factors for all nonhydrogen atoms. Hydrogen atoms were included as fixed, idealized contributors. For *paral*-[Fe(TMP)(5-MeHIm)$_2$]ClO$_4$, which crystallizes in the polar space group $P2_1$, the assignment of the enantiomer was made. The opposite hand yielded both weighted and unweighted R's that were 0.1% higher and the coordinates of the first hand are reported herein. Final discrepancy indices are listed in Table 1. Because of the unusual nature of *perp*-[Fe(TMP)(5-MeHIm)$_2$]ClO$_4$, a second structure determination of this form was undertaken using a new, independent crystal preparation. The structure was independently solved from this data set and carried through the refinement process until it was clear that the same structure had been obtained. Final atomic coordinates are listed in Tables S2 and S7. Fixed hydrogen atom coordinates and anisotropic temperature factors are given in the Supporting Information.

(40) Wagner, R. W.; Lawrence, D. S.; Lindsey, J. S. *Tetrahedron Lett.* **1987**, *28*, 3069−3070. Lindsey, J. S.; Wagner, R. W. *J. Org. Chem.* **1988**, *54*, 828−836.

(41) Adler, A. D.; Longo, F. R.; Kampas, F.; Kim, J. *J. Inorg. Nucl. Chem.* **1970**, *32*, 2443.

(42) Scheidt, W. R.; Turowska-Tyrk, I. *Inorg. Chem.* **1994**, *33*, 1314−1318.

(43) Programs used in this study included SHELXS-86: Sheldrick, G. M. *Acta Crystallogr., Sect. A* **1990**, *A46*, 467. Local modifications of Busing and Levy's ORFFE and ORFLS, Jacobson's ALLS, Zalkin's FORDAP, and Johnson's ORTEP2. Scattering factors were taken from: *International Tables for Crystallography*; Wilson, A. J. C., Ed.; Kluwer Academic Publishers: Dordrecht, 1992; Vol. C.

Low-Spin [Fe(TMP)(5-MeHIm)₂]ClO₄

J. Am. Chem. Soc., Vol. 121, No. 48, 1999 11147

Molecular Mechanics Calculations. These were performed on an IBM-compatible computer with our modified version[44] of Allinger's MM program MM2(87).[45] Input structures were either the X-ray structures of [Fe(TMP)(5-MeHIm)₂]ClO₄ (orthogonalized coordinates) or idealized structures with planar core conformations.[46] An energy cut-off for minimization of $\Delta U_T \leq 6.0 \times 10^{-5}$ kcal/mol between successive iterations was used with our previously described force field.[34,47,48] A dielectric constant of 10 D was used to take into account a fairly polar crystal environment. Partial atomic charges were not included in the calculations.[34,49,50]

The three X-ray structures of [Fe(TMP)(5-MeHIm)₂]ClO₄ were modeled by fixing the orientations of the axial ligands at their observed values using MM2's dihedral angle locking routine prior to refining all other structural parameters. Comparison of the energy-minimized and X-ray structures of [Fe(TMP)(5-MeHIm)₂]ClO₄ gave acceptable rmsd's (bond lengths, bond angles, torsion angles, 24-atom mean planes).

The orientation of an axial imidazole ligand relative to the porphyrin core may be defined by the torsion angle that involves a porphyrin nitrogen atom, the central metal ion, a coordinated axial imidazole nitrogen, and an imidazole α-carbon ($N_p-Fe-N_{ax}-C_{Im}$, ϕ). The orientations of a pair of trans imidazole ligands are then defined by the torsion angles ϕ_1 and ϕ_2, which are measured relative to the same porphyrin nitrogen.[51] Conformational surfaces for [Fe(TMP)(5-MeHIm)₂]⁺, [Fe(TPP)(5-MeHIm)₂]⁺, [Fe(porphine)(5-MeHIm)₂]⁺, and [Fe(TMP)(HIm)₂]⁺ were calculated by *counter-rotating* the axial ligands from 0 to 90° (ϕ_1) and 0 to 180° (ϕ_2) in 10° increments, producing a total of 10 × 19 starting conformations for refinement.[52] (This dihedral angle range maps the symmetry-unique portion of conformational space.) The method used by MM2 to fix the driven torsion angles during geometry optimization has been described elsewhere.[34] The strain energy components and coordination sphere structural parameters of the energy-optimized conformations were extracted from the MM2 output files and analyzed as a function of the driven torsion angles.

Results

[Fe(TMP)(5-MeHIm)₂]ClO₄ has been obtained in two crystalline forms with distinctly different molecular structures. The structures differ in the relative orientation of the axial ligands

(44) Munro, O. Q.; Bradley, J. C.; Hancock, R. D.; Marques, H. M.; Marsicano, F.; Wade, P. W. *J. Am. Chem. Soc.* **1992**, *114*, 7218−7230.

(45) (a) Allinger, N. L. *J. Am. Chem. Soc.* **1977**, *99*, 8127−8134. (b) Allinger, N. L.; Yuh, Y. MM2(87). Distributed to academic users by QCPE, under special agreement with Molecular Design Ltd., San Leandro, CA. (c) Sprague, J. T.; Tai, J. C.; Young, Y.; Allinger, N. L. *J. Comput. Chem.* **1987**, *8*, 581.

(46) ALCHEMY III, 3D Molecular Modeling Software. Tripos Associates Inc., 1699 S. Hanley Rd., St. Louis, MO. Other programs used in this study: (1) XANADU, program for manipulation of crystallographic data: Roberts, P.; Sheldrick, G. M. 1976/7. This program was routinely used to fit least-squares planes through the non-hydrogen atoms of the computed porphyrin cores. (2) AXUM, Technical Graphics and Data Analysis, V. 3.0. TriMetrix Inc., 444 NE Ravenna Boulevard, Suite 210, Seattle, WA 98115.

(47) Marques, H. M.; Munro, O. Q.; Grimmer, N. E.; Levendis, D. C.; Marsicano, F.; Pattrick, G.; Markoulides, T. *J. Chem. Soc., Faraday Trans.* **1995**, *91*, 1741−1749.

(48) The total steric energy of a given conformation, U_T, corresponds to the sum of the strain energy contributions from bond stretching/compression (U_b), angle-bending (U_θ), stretch-bend deformations (U_{SB}), 1,4-nonbonded interactions ($U_{1,4-NB}$), through-space nonbonded interactions (U_{NB}), torsion angle deformations (U_ϕ), and dipole−dipole interactions (U_μ).

(49) Shelnutt, J. A.; Medforth, C. J.; Berber, M. D.; Barkigia, K. M.; Smith, K. M. *J. Am. Chem. Soc.* **1991**, *113*, 4077−4087.

(50) The force field includes the standard MM2 bond dipoles for the C−C and C−N bonds. All M−L bond dipoles have an assigned value of zero.

(51) The orientations of imidazole and pyridine ligands in metalloporphyrin complexes are normally defined from crystallographic coordinates by the angle ϕ between the projection of the plane of the axial ligand onto the porphyrin core and the closest Fe−N_p vector.[53]

(52) Due to counter-rotation of the two torsion angles ϕ_1 and ϕ_2, a ϕ_2 value of +45°, for example, corresponds to an angle of − 45° in the frame of reference for ϕ_1.
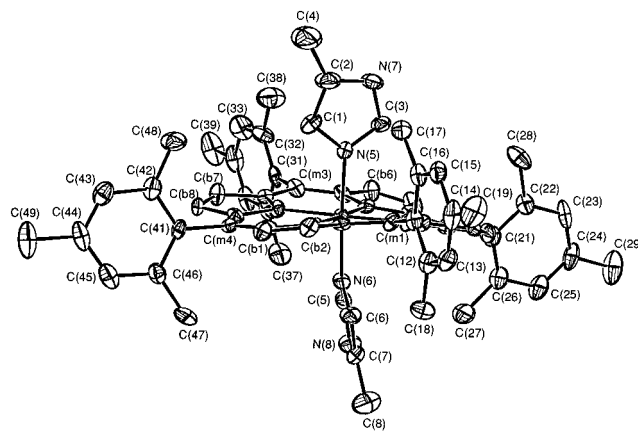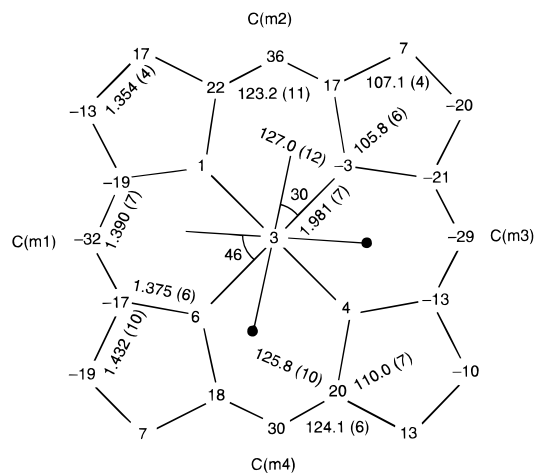

Figure 1. ORTEP diagram of *perp*-[Fe(TMP)(5-MeHIm)₂]ClO₄. Thermal ellipsoids are drawn at the 50% probability level. Hydrogen atoms are omitted for clarity.

and concomitant structural features. One form, which we denote as *perp*-[Fe(TMP)(5-MeHIm)₂]ClO₄, has the axial ligands in a relative perpendicular orientation; the second form (*paral*-[Fe(TMP)(5-MeHIm)₂]ClO₄) has the axial ligands in a relative parallel orientation. Both complexes have been characterized by single-crystal X-ray structure determinations and by Mössbauer and EPR spectroscopies. The structural results for *perp*-[Fe(TMP)(5-MeHIm)₂]ClO₄ are reported first, followed by those for *paral*-[Fe(TMP)(5-MeHIm)₂]ClO₄.

The molecular structure and numbering scheme for the crystallographically unique atoms of *perp*-[Fe(TMP)(5-MeHIm)₂]-ClO₄ are shown in the ORTEP diagram of Figure 1. The ORTEP diagram shows that *perp*-[Fe(TMP)(5-MeHIm)₂]ClO₄ has a near-perpendicular relative orientation of the axial imidazole ligands. The actual dihedral angle, $\Delta\phi$, between the two axial ligands is 76°. The projection of the two imidazole ligand planes onto the 24-atom porphyrin mean plane makes angles of 46° (ϕ_1) and 30° (ϕ_2) to the same Fe−N_p vector. (ϕ_1 denotes the orientation of the top ligand in all ORTEP diagrams.) The dihedral angles between the two ligand planes and the porphyrin plane are 82.4° and 77.5°. The dihedral angles between the four mesityl rings and the mean porphinato core are 82.0, 80.9, 84.3, and 84.2°.

Averaged values for the chemically equivalent bond distances and angles in the core are shown in the formal diagram of Figure 2. Also displayed are the individual displacement values of the crystallographically unique atoms from the mean plane of the 24-atom core (in units of 0.01 Å) and the orientation of the axial ligands. The porphinato core of *perp*-[Fe(TMP)(5-MeHIm)₂]-ClO₄ exhibits a modest degree of S_4-ruffling, in accord with observations for other [Fe^{III}(TMP)L₂]⁺ derivatives having axial ligands with relative perpendicular orientations. Also consistent with the ruffled core are the relatively short equatorial Fe−N_p bond distances which average to 1.981(7) Å and bending of the methine carbon atoms out of the plane of the individual pyrrole rings by an average of ±0.32 Å. The two independent axial bond distances (Fe^{III}−N_{ax}) are 1.973(6) and 1.957(6) Å. The axial N_{ax}−Fe−N_{ax} angle is 176.6(2)°; the N_{ax}−Fe−N_p angles range from 87.6(3) to 92.9(3)°. Selected values of the bond distances and bond angles in *perp*-[Fe(TMP)(5-MeHIm)₂]-ClO₄ are given in Table 2; complete listings of structural data are given in the Supporting Information.

The (uncoordinated) N−H groups of the two imidazole ligands of *perp*-[Fe(TMP)(5-MeHIm)₂]ClO₄ are within hydrogen bonding distance to oxygen atoms of the perchlorate anion. Distances are N(7)···O(2) = 2.872 Å and N(8)···O(4) = 2.842

Figure 2. Formal diagram of the porphinato core in *perp*-[Fe(TMP)-(5-MeHIm)$_2$]ClO$_4$ displaying the perpendicular displacement of each unique atom from the 24-atom mean plane. All displacements are given in units of 0.01 Å. The orientation of the axial ligands is given with the position of the methyl group of the imidazole indicated by the filled circle. Also entered on the diagram are the averaged values of all bond distances and angles of the core.

Table 2. Selected Bond Lengths and Bond Angles for *perp*-[Fe(TMP)(5-MeHIm)$_2$]ClO$_4$ and *paral*-[Fe(TMP)(5-MeHIm)$_2$]ClO$_4$

	perp-[Fe(P)L$_2$]-ClO$_4$[b]	*paral*-[Fe(P)L$_2$]-ClO$_4$(A)[c]	*paral*-[Fe(P)L$_2$]-ClO$_4$(B)[d]
	(A) bond lengths (Å)[a]		
Fe–N(1)	1.985(6)	1.986(5)	1.981(5)
Fe–N(2)	1.979(6)	1.978(5)	1.974(5)
Fe–N(3)	1.988(6)	1.985(5)	1.985(5)
Fe–N(4)	1.973(6)	1.984(5)	1.984(5)
Fe–N(5)	1.957(6)	1.978(6)	1.980(5)
Fe–N(6)/(7)[e]	1.973(6)	1.961(5)	1.985(5)
	(B) bond angles(°)		
N(1)–Fe–N(2)	91.16(24)	89.43(19)	90.44(19)
N(1)–Fe–N(3)	178.95(23)	179.19(21)	179.54(23)
N(1)–Fe–N(4)	89.07(24)	90.29(19)	89.87(19)
N(2)–Fe–N(3)	89.08(25)	90.30(19)	89.66(19)
N(2)–Fe–N(4)	179.52(25)	178.87(22)	178.85(23)
N(3)–Fe–N(4)	90.67(24)	90.00(19)	90.03(18)
N(5)–Fe–N(1)	88.38(23)	90.10(21)	89.98(21)
N(5)–Fe–N(2)	89.13(25)	90.79(22)	88.88(20)
N(5)–Fe–N(3)	90.60(24)	89.15(21)	89.58(21)
N(5)–Fe–N(4)	90.47(25)	90.31(21)	90.02(21)
N(6)/(7)[e]–Fe–N(1)	91.08(24)	90.08(21)	90.42(21)
N(6)/(7)[e]–Fe–N(2)	87.55(25)	89.14(21)	92.22(21)
N(6)/(7)[e]–Fe–N(3)	89.95(24)	90.67(21)	90.03(20)
N(6)/(7)[e]–Fe–N(4)	92.86(25)	89.77(21)	88.88(21)
N(6)/(7)[e]–Fe–N(5)	176.62(24)	179.80(22)	178.83(21)

[a] The estimated standard deviations of the least significant digits are given in parentheses. [b] P = TMP; L = 5-MeHIm. [c] Independent molecule A. [d] Independent molecule B. [e] Axial nitrogen trans to N(5) for molecules A and B of *paral*-[Fe(TMP)(5-MeHIm)$_2$]ClO$_4$.

Å. Hydrogen bonds of this sort (between the uncoordinated N–H group and the counteranion) are frequently observed in porphinatoiron(III) imidazole complexes with N–H groups.

The crystal structure of *paral*-[Fe(TMP)(5-MeHIm)$_2$]ClO$_4$ consists of two independent molecules in the asymmetric unit which we denote as molecule A and molecule B; the molecular structures of both are shown in the ORTEP diagrams of Figure 3. The numbering schemes for the crystallographically unique atoms are also displayed. The ORTEP diagrams show that the imidazole ligands are arranged in nearly parallel orientation for both molecules. The dihedral angles, Δϕ, between the two axial ligands are 30° for molecule A and 26° for molecule B. The projection of the two ligand planes onto the 24-atom porphyrin
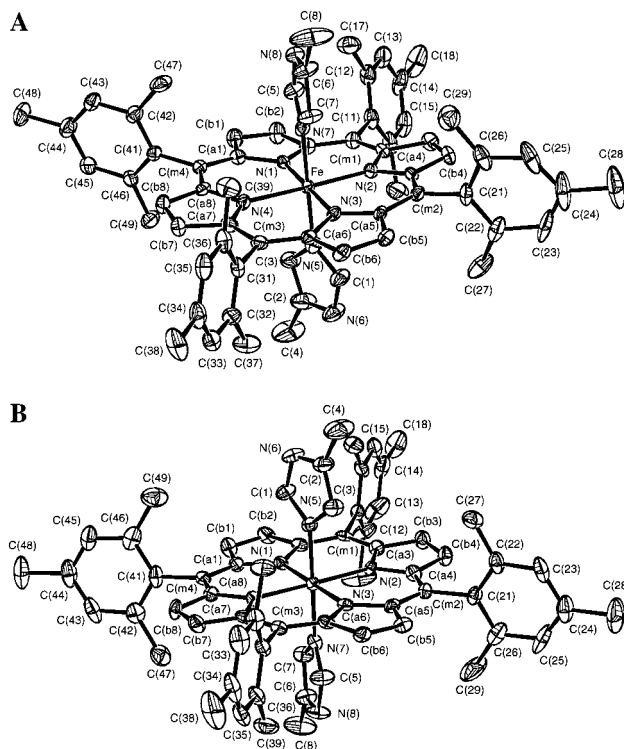

Figure 3. ORTEP diagram of *paral*-[Fe(TMP)(5-MeHIm)$_2$]ClO$_4$ for Molecule A and Molecule B. Thermal ellipsoids are drawn at the 50% probability level. Hydrogen atoms are omitted for clarity.

mean plane makes dihedral angles of 10° (ϕ_1) and 20° (ϕ_2) to the closest Fe–N$_p$ vector for molecule A, and angles of 14° (ϕ_1) and 12° (ϕ_2) for molecule B. The dihedral angles between the ligand planes and the porphyrin plane are 86.0° and 88.3° (molecule A), and 83.2° and 86.6° (molecule B). The dihedral angles between the four mesityl rings and the 24-atom porphyrin mean plane are 77.3, 85.8, 89.5, and 86.0° for molecule A; those for molecule B are 86.1, 88.4, 87.2, and 78.9°.

Figure 4 shows the perpendicular displacements of the crystallographically unique atoms from the mean planes of the 24-atom porphyrin cores (in units of 0.01 Å) of molecules A and B of *paral*-[Fe(TMP)(5-MeHIm)$_2$]ClO$_4$ and the orientation of the axial ligands. Averaged values for the chemically equivalent bond distances and angles of the porphyrin core are displayed in each formal diagram. *paral*-[Fe(TMP)(5-MeHIm)$_2$]-ClO$_4$ has a relatively planar porphinato core; molecule B is more planar than molecule A. The Fe–N$_{ax}$ distances for molecule A are 1.978(6) and 1.961(5) Å; those for molecule B are 1.980(5) and 1.985(5) Å. Equatorial bond distances (Fe–N$_p$) average to 1.983(4) Å for molecule A and 1.981(5) Å for molecule B. The N$_{ax}$–Fe–N$_{ax}$ angle is 179.80(22)° (molecule A) and 178.83-(21)° (molecule B); the N$_{ax}$–Fe–N$_p$ angles range from 89.14-(21)° to 90.79(22)° (molecule A) and 88.88(21)° to 92.22(21)° (molecule B). Selected values of the bond distances and bond angles for both molecules are given in Table 2; complete listings of structural data are given in the Supporting Information.

The N–H groups of all imidazole ligands of both *paral*-[Fe-(TMP)(5-MeHIm)$_2$]$^+$ ions are within hydrogen bonding distance of acceptors in the solid-state structure. One imidazole N–H of each cation is hydrogen bonded to an oxygen atom of the perchlorate anions. Distances are N(6)A···O(1) = 2.929 Å and N(6)B···O(5) = 2.866 Å. The N–H of the other imidazole of each molecule is involved in a much stronger hydrogen bond in which the acceptors are the unprotonated nitrogen atoms of the solvate 4(5)MeHIm molecules. The N(8)A···N(4)S and

A

B
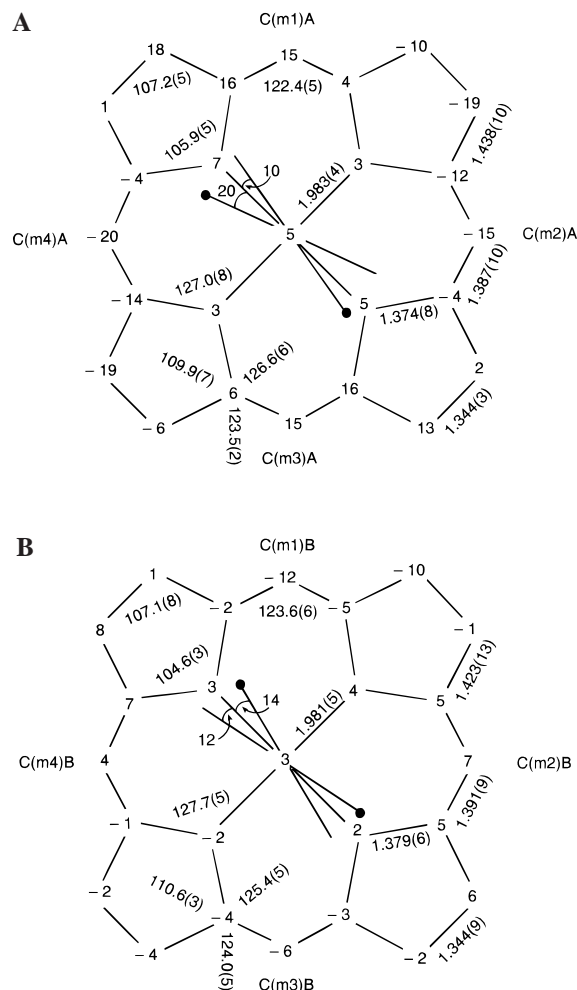
Figure 4. Formal diagram of the porphinato core in *paral*-[Fe(TMP)-(5-MeHIm)₂]ClO₄ for Molecule A and Molecule B displaying the perpendicular displacement of each unique atom from the 24-atom mean plane. All displacements are given in units of 0.01 Å. The orientation of the axial ligands is given with the position of the methyl group of the imidazole indicated by the filled circle. Also entered on the diagram are the averaged values of all bond distances and angles of the core.

N(8)B···N(2)S distances are 2.715 and 2.846 Å. These distances are indicative of relatively strong hydrogen bonds. The solvate imidazole molecules are further involved in a three-dimensional hydrogen bonding network. A complete tabulation of the hydrogen bonding distances is available in Table S12 of the Supporting Information.

The Mössbauer spectrum of polycrystalline *perp*-[Fe(TMP)-(5-MeHIm)₂]ClO₄ taken at 120 K is shown in Figure S2a. The spectrum shows a quadrupole doublet with a small splitting (ΔE_q) of 1.78(1) mm/s and an isomer shift (δ) of 0.22(1) mm/s. The values of the quadrupole splitting and isomer shift are consistent with other low-spin iron(III) porphyrinates with the axial ligands in a relative perpendicular orientation.[15,19] The EPR spectrum of a polycrystalline sample of *perp*-[Fe(TMP)(5-MeHIm)₂]ClO₄ recorded at 4.2 K is shown in Figure 5a. A single feature with $g_{max} = 3.43$ is observed for the majority species; very minor contamination of the sample by two rhombic low-spin iron(III) species ($g_1 = 2.90$ and 2.77; $g_2 = 2.21$) and a high-spin iron(III) species ($g_\perp = 6.03$) is also evident. The "large g_{max}" signal from *perp*-[Fe(TMP)(5-MeHIm)₂]ClO₄ is consistent with near-degeneracy of the d$_{xz}$ and d$_{yz}$ orbitals (near-axial
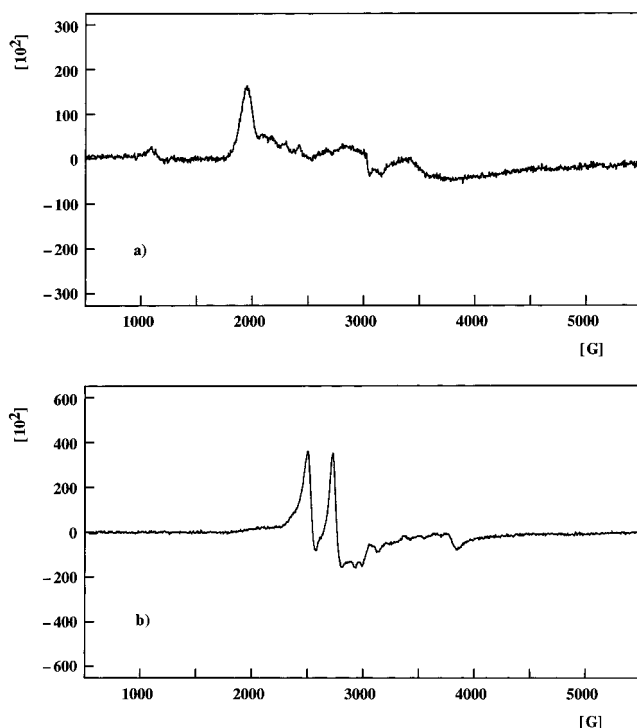
Figure 5. X-band EPR spectra of (a) *perp*-[Fe(TMP)(5-MeHIm)₂]ClO₄ and (b) *paral*-[Fe(TMP)(5-MeHIm)₂]ClO₄ at 4.2 K.

electronic symmetry) and a relative perpendicular axial ligand orientation.[15,19,54]

The Mössbauer spectrum of *paral*-[Fe(TMP)(5-MeHIm)₂]-ClO₄ taken at 120 K is shown in Figure S2b. The spectrum reveals a quadrupole doublet with a splitting (ΔE_q) of 2.56(1) mm/s and an isomer shift (δ) of 0.22(3) mm/s. The values for the quadrupole splitting are representative of other low-spin iron-(III) porphyrinates with axial imidazoles and pyridines in a relative parallel orientation.[15,19] The EPR spectrum of a polycrystalline sample of *paral*-[Fe(TMP)(5-MeHIm)₂]ClO₄ taken at 4.2 K (Figure 5b) displays a rhombic **g** tensor with *g*-values of 2.69, 2.34−2.43, and 1.75, consistent with similar systems that have relative parallel axial ligand orientations.[13,15,16,37] There is some apparent variation in the position of the central line of the spectrum, but the two outer features remain at the same field positions as the EPR tube is rotated.

MM-calculated and crystallographically observed bond distances, bond angles, and torsion angles for the three structures of [Fe(TMP)(5-MeHIm)₂]⁺ are compared in Table S13. The mean differences between the calculated and observed structural parameters are 0.016 Å (bond distances), 1.8° (bond angles), and ∼5° (torsion angles) for the three structures. Figure 6 compares the calculated and observed conformations of the three [Fe(TMP)(5-MeHIm)₂]⁺ cations;[55] the average absolute displacements of the various classes of porphyrin core atoms from the porphyrin mean plane are compared in Table 3. The S₄-ruffled structure of *perp*-[Fe(TMP)(5-MeHIm)₂]⁺ is well modeled. However, the calculated conformations of *paral*-[Fe(TMP)-(5-MeHIm)₂]⁺ are somewhat more ruffled than the X-ray structures. The near-orthogonal dihedral angles between the planes of the axial imidazole ligands and the porphyrin mean plane are reproduced in the two calculated structures of *paral*-

(53) Scheidt, W. R.; Lee, Y. J. *Struct. Bonding* **1987**, *64*, 1−70.

(54) Palmer, G. *Biochem. Soc. Trans.* **1985**, *13*, 548−560.

(55) The rmsd's for the fits are: *perp*-[Fe(TMP)(5-MeHIm)₂]ClO₄, 0.085 Å; *paral*-[Fe(TMP)(5-MeHIm)₂]ClO₄ (molecule A), 0.086 Å; and *paral*-[Fe(TMP)(5-MeHIm)₂]ClO₄ (molecule B), 0.091 Å.

11150   *J. Am. Chem. Soc., Vol. 121, No. 48, 1999*

Munro et al.

Table 3. Comparison of Crystallographically Observed and Calculated Core Conformations for [Fe(TMP)(5-MeHIm)$_2$]ClO$_4$[a]

	perp-[Fe(TMP)-(5-MeHIm)$_2$]$^+$		paral-[Fe(TMP)-(5-MeHIm)$_2$]$^+$ A[b]		paral-[Fe(TMP)-(5-MeHIm)$_2$]$^+$ B[c]	
	obs[d]	calc[d]	obs[e]	calc[e]	obs[f]	calc[f]
|Fe|	3	1	5	1	3	0
|N$_4$|	4(2)	3(2)	4(2)	3(1)	2(1)	1(1)
|C$_a$|	18(3)	20(7)	10(6)	14(3)	4(2)	12(1)
|C$_b$|	13(5)	15(14)	11(8)	9(4)	4(3)	8(2)
|C$_m$|	32(3)	38(1)	16(3)	27(1)	7(3)	24(1)
|C$_{20}$|	19(8)	21(13)	12(6)	15(7)	5(3)	13(6)
|C$_{20}$N$_4$Fe|	16(10)	18(14)	10(6)	12(8)	4(3)	11(7)

[a] |C$_a$|, |C$_b$|, |C$_m$|, |C$_{20}$|, |N$_4$|, |C$_{20}$N$_4$Fe|, and |Fe| are the mean absolute displacements of the α-, β-, *meso*-, 20-porphyrin carbons, pyrrole nitrogens, all atoms, and iron from the mean plane of the porphyrin (in units of 0.01 Å), respectively. [b] Molecule A. [c] Molecule B. [d] $\phi_1 = -42.8°$, $\phi_2 = -35.3°$. [e] $\phi_1 = -6.4°$, $\phi_2 = 159.0°$. [f] $\phi_1 = 8.4°$, $\phi_2 = -167.4°$.
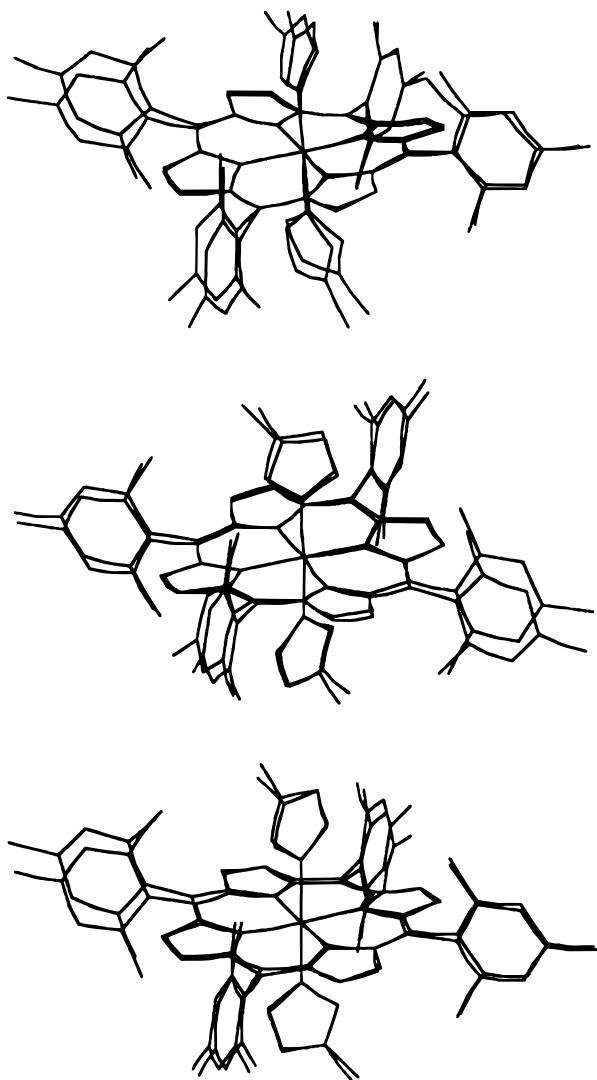
Figure 6. Comparison of calculated and crystallographically observed structures of [Fe(TMP)(5-MeHIm)$_2$]ClO$_4$. The X-ray structures to which the calculated structures have been fitted are, from top to bottom, *perp*-[Fe(TMP)(5-MeHIm)$_2$]ClO$_4$, *paral*-[Fe(TMP)(5-MeHIm)$_2$]ClO$_4$ (molecule A), and *paral*-[Fe(TMP)(5-MeHIm)$_2$]ClO$_4$ (molecule B). Hydrogen atoms have been omitted for clarity.

[Fe(TMP)(5-MeHIm)$_2$]$^+$ (Figure 6). However, the tilt of the axial ligands observed in the X-ray structure of *perp*-[Fe(TMP)-(5-MeHIm)$_2$]$^+$ is not well modeled.

Figure 7 compares conformational surfaces for [Fe(TMP)-(5-MeHIm)$_2$]$^+$ and [Fe(TPP)(5-MeHIm)$_2$]$^+$ as plots of the change in total steric energy (relative to the global minimum) as a function of the orientations (ϕ_1 and ϕ_2) of the axial imidazole ligands relative to one of the four equivalent porphyrin nitrogens. A three-dimensional surface and a map of the surface are shown for each complex. The minimum energy conformation of [Fe(TMP)(5-MeHIm)$_2$]$^+$ occurs at ϕ_1, $\phi_2 = 45°$; the axial ligands have a relative perpendicular orientation and the porphyrin core is S_4-ruffled. A strain energy maximum occurs at ϕ_1, $\phi_2 = 45°$, $135°$ when the axial ligands adopt a relative parallel orientation over a planar porphyrin core and point directly toward the *meso*-mesityl groups. In the case of [Fe-(TPP)(5-MeHIm)$_2$]$^+$, a local minimum is observed at ϕ_1, $\phi_2 = 45°$, $135°$ in addition to the global minimum at ϕ_1, $\phi_2 = 45°$. The locations of two of the three X-ray structures of [Fe(TMP)-(5-MeHIm)$_2$]ClO$_4$ are shown by the arrows on the map of the conformational surface for [Fe(TMP)(5-MeHIm)$_2$]$^+$. The X-ray structure of *perp*-[Fe(TMP)(5-MeHIm)$_2$]ClO$_4$ lies close to the calculated lowest energy conformation (point **2**). The X-ray structure of *paral*-[Fe(TMP)(5-MeHIm)$_2$]$^+$ (molecule A) is found in a region of higher steric strain at point **1**.[56]

Varying the relative orientations of the axial 5-MeHIm ligands of [Fe(TMP)(5-MeHIm)$_2$]$^+$ leads to significant conformational changes (Figure 7) as well as structural changes in the iron(III) coordination sphere (Figure 8). In Figure 8a, the S_4-ruffled conformation of [Fe(TMP)(5-MeHIm)$_2$]$^+$ (ϕ_1, $\phi_2 = 45°$) is calculated to have shorter Fe–N$_p$ bonds (~1.967 Å) than the planar conformation (ϕ_1, $\phi_2 = 45°$, $135°$; average Fe–N$_p$ distance ~1.984 Å). From Figure 8b, the difference in the average bond length, Δ_{xy}, for the two pairs of trans Fe–N$_p$ bonds is zero when the axial ligands have a relative perpendicular orientation and are positioned over the Fe–N$_p$ bonds (ϕ_1, $\phi_2 = 0°$, $90°$), or over the methine carbons (ϕ_1, $\phi_2 = 45°$). A maximum difference (0.011 Å) is observed when the axial ligands are slightly staggered and nearly eclipse one pair of trans Fe–N$_p$ bonds (ϕ_1, $\phi_2 = 18°$, $162°$). The average Fe–N$_{ax}$ distance also varies with axial ligand orientation (Figure 8c). The axial bonds are calculated to be longest (~1.981 Å) when the 5-MeHIm ligands eclipse a trans pair of Fe–N$_p$ bonds and have a relative parallel orientation (ϕ_1, $\phi_2 = 0°$); the shortest average Fe–N$_{ax}$ distance (~1.958 Å) is observed when the axial ligands adopt a relative perpendicular orientation and point toward the porphyrin meso carbons (S_4-ruffled conformation).

Discussion

Molecular Structures. The structures of [Fe(TMP)(5-MeHIm)$_2$]ClO$_4$ are remarkable in several respects. Most importantly, they represent the first example of a low-spin iron(III) porphyrin complex with two different relative orientations for the same pair of axial ligands. The two crystalline forms of [Fe(TMP)(5-MeHIm)$_2$]ClO$_4$ have distinctly different EPR and Mössbauer spectroscopic parameters which allow us to definitively correlate the electronic structure of the iron(III) ion with the relative orientations of the axial imidazole ligands.

Bis-imidazole complexes of low-spin iron(III) porphyrins with relative perpendicular axial ligand orientations and S_4-ruffled core conformations are normally observed with bulky axial ligands, for example, [Fe(TPP)(2-MeHIm)$_2$]ClO$_4$,[18] [Fe(TMP)-

(56) The location of the X-ray structure of *paral*-[Fe(TMP)(5-MeHIm)$_2$]-ClO$_4$ (molecule B) on the conformational surface is related to the position for molecule A (point **1**) by an approximate two-fold rotation about an axis orthogonal to the map in Figure 7 centered at ϕ_1, $\phi_2 = 0°$.
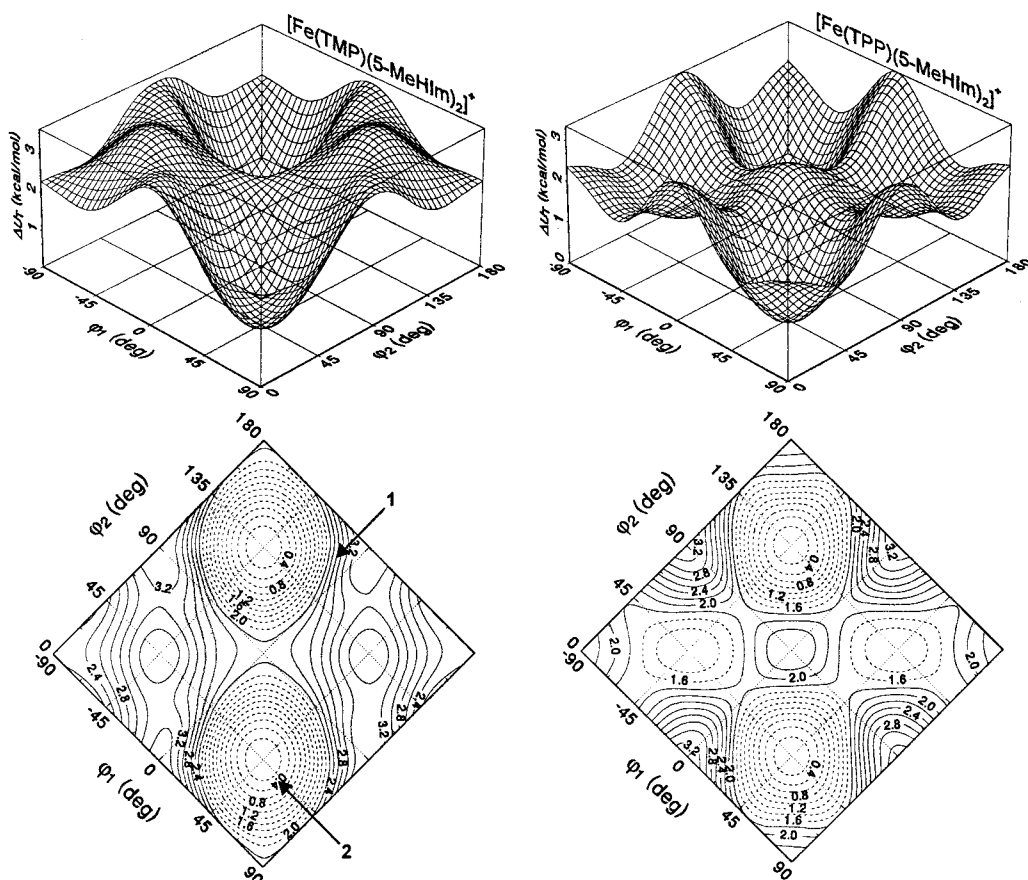
Figure 7. Plot of the change in steric energy (ΔU_T) as a function of axial 5-MeHIm orientation for [Fe(TMP)(5-MeHIm)₂]⁺ and [Fe(TPP)(5-MeHIm)₂]⁺. A contour map of the three-dimensional surface is shown in each case. ϕ_1 and ϕ_2 correspond to the torsion angles N_p–Fe–N_{ax}–C_{Im} for the top and bottom ligands, respectively. The locations of the X-ray structures of [Fe(TMP)(5-MeHIm)₂]ClO₄ on the conformational surface are shown: point **1**, *paral*-[Fe(TMP)(5-MeHIm)₂]ClO₄ (molecule A); point **2**, *perp*-[Fe(TMP)(5-MeHIm)₂]⁺.

(1,2-Me₂Im)₂]ClO₄,[34] and [Fe(TMP)(BzHIm)₂]ClO₄.[57] The structure of *perp*-[Fe(TMP)(5-MeHIm)₂]ClO₄ is unusual since the axial ligands are staggered and the porphyrin S_4-ruffled, even though the 5-MeHim ligands are not particularly bulky. The conformation of *perp*-[Fe(TMP)(5-MeHIm)₂]ClO₄ is therefore similar to Hoard's structure of [Fe(TPP)(HIm)₂]Cl.[58] Both derivatives display staggered imidazole orientations and quasi S_4-ruffled porphyrin cores. However, the dihedral angle between the 5-MeHIm groups of *perp*-[Fe(TMP)(5-MeHIm)₂]ClO₄ (76°) is closer to 90° than the dihedral angle (57°) between the two imidazole ligands of [Fe(TPP)(HIm)₂]Cl.[58] The porphinato core of *perp*-[Fe(TMP)(5-MeHIm)₂]ClO₄ ($|C_m|$ = 0.32 (3) Å) exhibits a similar magnitude of S_4-ruffling to that of [Fe(TPP)-(HIm)₂]Cl ($|C_m|$ = 0.31 (3) Å). The average Fe–N_p bond lengths for the two complexes (1.981(7) Å for *perp*-[Fe(TMP)-(5-MeHIm)₂]ClO₄ and 1.989(5) Å for [Fe(TPP)(HIm)₂]Cl[58]) are, within the estimated uncertainties, equivalent. This reflects the similar degree of S_4-ruffling observed in the two complexes. However, the mean Fe–N_p bond length for *perp*-[Fe(TMP)(5-MeHIm)₂]ClO₄ is notably shorter than that typical for planar low-spin iron(III) porphyrins (~1.990 Å),[59] consistent with moderate S_4-ruffling of the porphyrin.

In contrast to [Fe(TPP)(HIm)₂]Cl,[58] the axial imidazoles of *perp*-[Fe(TMP)(5-MeHIm)₂]ClO₄ are tilted (by 12.5° and 7.6°,

respectively) from the plane of the heme normal. Such tilting is not without precedent. Structurally characterized examples of off-axis imidazole coordination in low-spin iron(III) porphyrins include [Fe(TMP)(1-MeIm)₂]ClO₄ (6.3° and 1.2°),[15] [Fe-(TPP)(*t*-MU)₂]SbF₆ (4°),[37] and [Fe(TPP)(HIm)₂]Cl (3.6° and 3.0°).[16] Obviously, the tilt angle of *perp*-[Fe(TMP)(5-MeHIm)₂]-ClO₄ is larger than the listed cases. Crystal packing effects and/or hydrogen bonding to the N–H proton of coordinated imidazoles may influence whether the ligands bind in an off-axis manner since not all mono- and bis-imidazole complexes show this type of distortion. Off-axis binding of imidazole-(histidine) ligands has also been seen in a number of heme protein derivatives.

The Fe–N_{ax} bond lengths of *perp*-[Fe(TMP)(5-MeHIm)₂]-ClO₄ are significantly different; the bond to the 5-MeHIm ligand with ϕ_1 = 46° (1.957(6) Å) is shorter than the bond (1.973(6) Å) to the trans ligand with ϕ_2 = 30°. This trend of longer Fe–N_{ax} bonds for smaller values of ϕ has been observed in other bis-imidazole iron(III) porphyrinates,[16,37,58,60] including the present structure of *paral*-[Fe(TMP)(5-MeHIm)₂]ClO₄ (molecule A). As pointed out by Hoard,[58] lengthening of the Fe–N_{ax} bonds as $\phi \rightarrow 0°$ reflects increased nonbonded repulsion between the α-hydrogens of the axial ligands and the porphinato nitrogens. However, it is noteworthy that the value of ϕ is *not* a quantitative indicator of axial bond length in these complexes.[53]

The axial ligands of *paral*-[Fe(TMP)(5-MeHIm)₂]ClO₄ adopt a relative parallel orientation. However, the 5-MeHIm groups are somewhat staggered rather than exactly eclipsed; $\Delta\phi$ = 30°

(57) The structure of [Fe(TMP)(BzHIm)₂]ClO₄ has an S_4-ruffled porphyrin core and a relative perpendicular arrangement of the axial ligands ($\Delta\phi$ = 89°). Serth-Guzzo, J. A.; Turowska-Tyrk, I.; Scheidt, W. R. Manuscript in preparation.

(58) Collins, D. M.; Countryman, R.; Hoard, J. L. *J. Am. Chem. Soc.* **1972**, *94*, 2066–2072.

(59) Scheidt, W. R.; Reed, C. A. *Chem. Rev.* **1981**, *81*, 543–555.

(60) Little, R. G.; Dymock, K. R.; Ibers, J. A. *J. Am. Chem. Soc.* **1975**, *97*, 4532–4539.
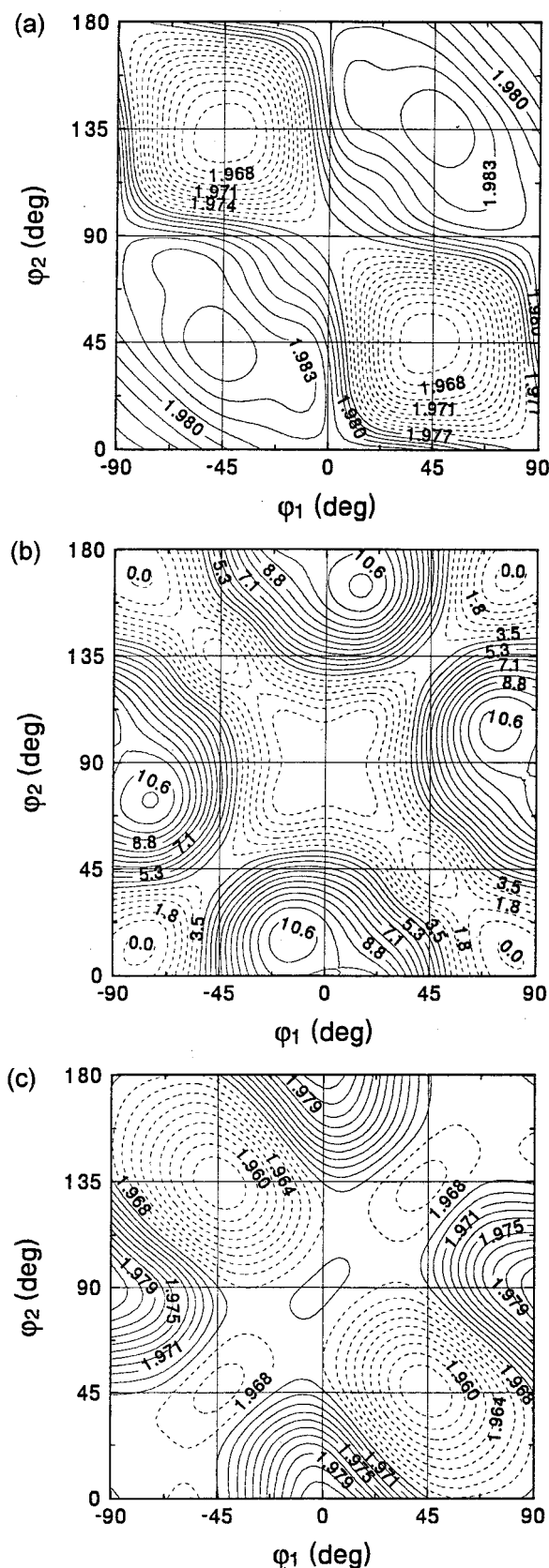
Figure 8. Contour maps of (a) the average $Fe-N_p$ bond distance, (b) the difference between the mean $Fe-N_p$ bond distance along the x- and y-directions of the heme group, Δ_{xy}, and (c) the average $Fe-N_{ax}$ bond distance with the orientation of the axial 5-MeHIm ligands for $[Fe(TMP)(5\text{-}MeHIm)_2]^+$.

for molecule A and 26° for molecule B. Moreover, the projections of the axial ligand planes onto the porphyrin core

relative to the closest $Fe-N_p$ bond differ for the two molecules (10 and 20° for molecule A, 12 and 14° for molecule B). Interestingly, the porphyrin cores of both molecules show a modest degree of S_4-ruffling, with molecule A ($|C_m| = 0.16(3)$ Å) somewhat more distorted than molecule B ($|C_m| = 0.07(3)$ Å). The nonplanar porphyrin cores of the two structures of *paral*-$[Fe(TMP)(5\text{-}MeHIm)_2]ClO_4$ (Figures 2 and 4) clearly reflect the different axial ligand orientations in each case, particularly since the dihedral angles between the porphyrin mean plane and mesityl groups are similar for both molecules.

A small staggering of near-parallel axial imidazoles has been observed in other low-spin iron(III) porphyrinates, indeed all those for which inversion symmetry at the metal is not crystallographically required. Thus, $\Delta\phi$ is 11° in $[Fe(TPP)(1\text{-}MeIm)_2]ClO_4$, 6° in $[Fe(T\text{-}2,6\text{-}Cl_2PP)(1\text{-}VinIm)_2]ClO_4$, and 13° in $[Fe(Proto\ IX)(1\text{-}MeIm)_2]$. Interestingly, the porphyrin cores of each exhibit modest distortions which appear to reflect (i) the orientations of the axial ligands relative to the $Fe-N_p$ bonds and (ii) the orientations of the *meso*-aryl groups relative to the porphyrin mean plane (TPP and T-2,6-Cl$_2$PP derivatives). However, the contribution made by nonbonded interactions between the *meso*-mesityl groups and pyrrole rings to possible nonplanar distortions of the porphyrin core in both molecules of *paral*-$[Fe(TMP)(5\text{-}MeHIm)_2]ClO_4$ is small since the mesityl rings are not tilted to angles <77° relative to the heme plane.

Finally, the dispersion in the $Fe-N_p$ bond distances for molecules A and B of *paral*-$[Fe(TMP)(5\text{-}MeHIm)_2]ClO_4$ is small. There is no experimental evidence for an in-plane rhombic distortion (shorter $Fe-N_p$ bonds perpendicular to the mean plane of the axial imidazoles; longer $Fe-N_p$ bonds parallel to the mean plane of the axial imidazoles) for either molecule. This might have been expected given the structural data for analogous complexes with relative parallel axial ligand orientations, for example, $[Fe(TMP)(1\text{-}MeIm)_2]ClO_4$ (molecule 1),[15] $[Fe(TPP)\text{-}(1\text{-}MeIm)_2]ClO_4$,[17] $[Fe(TPP)HIm_2]Cl$ (molecule A),[16] and $[Fe\text{-}(TPP)(c\text{-}MU)_2]SbF_6$ (molecule B),[37] all of which show this type of distortion. However, all have more planar porphyrin cores than molecules A and B of *paral*-$[Fe(TMP)(5\text{-}MeHIm)_2]ClO_4$ and, with the exception of $[Fe(TPP)(1\text{-}MeIm)_2]ClO_4$,[17] each displays a value of $\Delta\phi = 0°$. Clearly, the conformation of the porphyrin and the magnitude of $\Delta\phi$ may determine whether an in-plane rhombic distortion in the $Fe-N_p$ bonds is observed, especially since such distortions are probably related, in part, to imidazole $p\pi$−iron(III) d_{yz} π-bonding[17] which is at a maximum when $\Delta\phi = 0°$. Interestingly, the average $Fe-N_p$ bond distances of 1.983(4) Å for molecule A and 1.981(5) Å for molecule B of *paral*-$[Fe(TMP)(5\text{-}MeHIm)_2]ClO_4$ are shorter than the nominal distance of 1.990 Å for planar low-spin iron-(III) porphyrins.[59] This undoubtedly reflects the small S_4-ruffling displayed by each molecule. It is nonetheless surprising that *perp*-$[Fe(TMP)(5\text{-}MeHIm)_2]ClO_4$, with the most ruffled core conformation, has a mean $Fe-N_p$ distance equivalent to that of molecule B of *paral*-$[Fe(TMP)(5\text{-}MeHIm)_2]ClO_4$.

Why have we been able to isolate two crystalline forms of $[Fe(TMP)(5\text{-}MeHIm)_2]ClO_4$ with differing relative axial ligand orientations? Previous studies strongly suggest that the preferred relative ligand orientation for bis(imidazole)iron(III) porphyrinates, in the absence of introduced steric effects, is the parallel orientation. The solid-state structure of *paral*-$[Fe(TMP)(5\text{-}MeHIm)_2]ClO_4$ is observed to be in a hydrogen-bonding network and this feature might be considered responsible for the parallel orientation of the axial ligands. However, the observation of solution-state, rhombic EPR spectra under conditions where hydrogen bonding can not be present as well as when it is

present (vide infra) suggests that the observed solid-state H-bonding is not required for the parallel ligand orientation for this ligand combination. Thus an explanation of why the relative perpendicular orientation can be observed must be sought. The preparation of crystalline *perp*-[Fe(TMP)(5-MeHIm)₂]ClO₄ requires the presence of an "impurity" ligand, the weakly basic, strong π-accepting ligand 4-cyanopyridine as well as 4(5)-MeHIm. Similar ligand combinations can give rise to a mixed ligand complex in which pyridine and imidazole have a relative perpendicular orientation.[61] In the current circumstances, we believe that a small amount of a mixed ligand complex with relative perpendicular orientations provides a template for the crystallization of *perp*-[Fe(TMP)(5-MeHIm)₂]ClO₄. It is to be emphasized that the procedure described is quite reproducible, even if empirical.

EPR and Mössbauer Spectroscopy. The EPR spectrum of polycrystalline *perp*-[Fe(TMP)(5-MeHIm)₂]ClO₄ is of the "large g_{max}" spectral type,[14] consistent with a near perpendicular arrangement for the axial 5-MeHIm groups[15,19] and near-degeneracy of the d_{xz} and d_{yz} orbitals in a $(d_{xy})^2(d_{xz},d_{yz})^3$ ion. The value of g_{max} (3.43) is bracketed by the *g*-values reported for polycrystalline samples of [Fe(TPP)(2-MeHIm)₂]ClO₄ (g_{max} = 3.56)[18] and [Fe(TMP)(2-MeHIm)₂]ClO₄ (g_{max} = 3.17),[19] both of which have relative perpendicular axial ligand orientations.[62] Moreover, several structurally characterized bis-pyridine derivatives with relative perpendicular axial ligand orientations, including [Fe(TMP)(4-NMe₂Py)₂]ClO₄ (g_{max} = 3.48)[15] and [Fe(TMP)(4-NH₂Py)₂]ClO₄ (g_{max} = 3.40),[19] have g_{max}-values bracketing those of the g_{max} of *perp*-[Fe(TMP)(5-MeHIm)₂]-ClO₄. It is interesting that the large g_{max} spectral type is observed and is not significantly different in *g*-value from the bis-ligand complexes having dihedral angles of very close to 90°, when the dihedral angle of *perp*-[Fe(TMP)(5-MeHIm)₂]ClO₄ is only 76°.

Effective axial electronic symmetry at the metal occurs when the rhombic splitting, *V*, is much smaller than the tetragonality, Δ.[63] An important consequence is that the electric field gradient (EFG) at the iron nucleus is reduced below the single-electron value and smaller quadrupole splittings (ΔE_q < 2.0 mm/s)[15,19,64] are observed in the ^{57}Fe Mössbauer spectra of such species. In contrast, ΔE_q values >2.0 are consistent with a relative parallel axial ligand orientation. The relative orientations of the axial ligands in bis-imidazole iron(III) porphyrinates may therefore be assigned from a Mössbauer spectrum taken under conditions of small applied magnetic field. Together with EPR and structural data, a definitive correlation between the relative orientations of the axial ligands and the electronic structure of the metal may be established. In the case of *perp*-[Fe(TMP)-(5-MeHIm)₂]ClO₄, the small Mössbauer quadrupole splitting (ΔE_q = 1.78(1) mm/s) and "large g_{max}" EPR spectral type provide unambiguous evidence that a relative perpendicular axial ligand orientation leads to near degeneracy of the d_{xz} and d_{yz} orbitals.

(61) Scheidt, W. R.; Serth-Guzzo, J.; Turowska-Tyrk, I.; Safo, M. K.; Walker, F. A.; Debrunner, P. G. *Abstracts of Papers*; 208th National Meeting of the American Chemical Society, Washington, D. C., Aug 21−25, 1994; American Chemical Society: Washington, D.C., 1994; INORG 376.

(62) The X-ray structure of [Fe(TMP)(2-MeHIm)₂]ClO₄ has not been determined. However, the ¹H NMR spectrum of this species suggests an S_4-ruffled porphyrin conformation in solution at −74 °C.[38]

(63) Values of *V* and Δ were calculated following Taylor. Taylor, C. P. S. *Biochim. Biophys. Acta* **1977**, *491*, 137−148. We have assumed that "*z*" is along the heme normal to calculate the ligand field parameters.

(64) (a) Medhi, O. K.; Silver, J. *J. Chem. Soc., Dalton Trans.* **1990**, 263−270. (b) Medhi, O. K.; Silver, J. *J. Chem. Soc., Dalton Trans.* **1990**, 555−559.
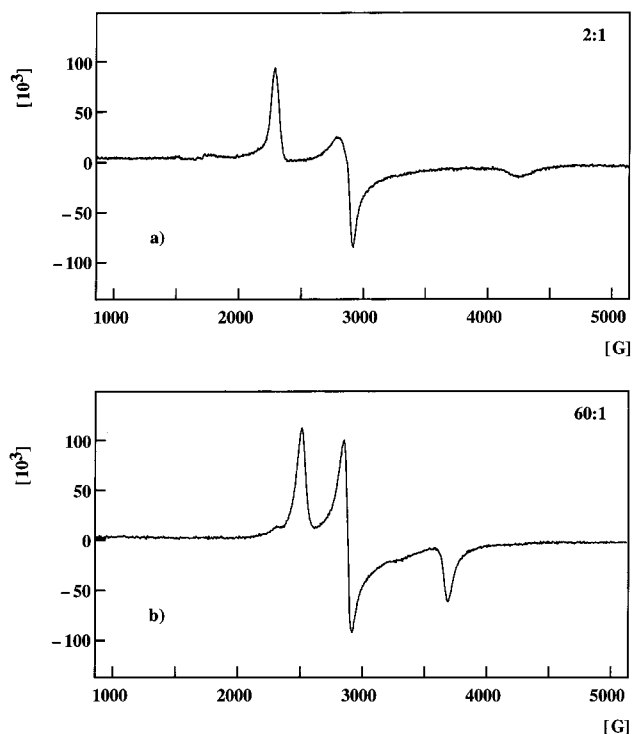
Figure 9. X-band EPR spectra of [Fe(TMP)(5-MeHIm)₂]ClO₄ in 3:1 DMF−acetonitrile glasses at 4.2 K. The top spectrum has an imidazole−Fe ratio of 2:1; the bottom panel has an imidazole−Fe ratio of 60:1.

The EPR *g*-values for *paral*-[Fe(TMP)(5-MeHIm)₂]ClO₄ (g_1 = 2.69, g_2 = 2.34−2.43, and g_3 = 1.75) show a smaller spread than the range found for other structurally characterized low-spin bis-imidazole iron(III) porphyrinates with relative parallel axial ligand orientations, including various cytochromes b_5 (g_1 = 3.03−3.07, g_2 = 2.22−2.24, g_3 = 1.35−1.46, V/λ = 1.55−1.71, Δ/λ = 3.00−3.32, V/Δ = 0.51−0.52),[65] [Fe(TMP)(1-MeIm)₂]ClO₄ (g_1 = 2.886, g_2 = 2.325, g_3 = 1.571; V/λ = 2.07, Δ/λ = 3.09, V/Δ = 0.67),[15] [Fe(TPP)(HIm)₂]Cl (g_1 = 2.84, g_2 = 2.32, g_3 = 1.59; V/λ = 2.16, Δ/λ = 3.12, V/Δ = 0.69),[16] and [Fe(TPP)(1-MeIm)₂]ClO₄ (g_1 = 2.866, g_2 = 2.276, g_3 = 1.535, V/λ = 2.01, Δ/λ = 3.16, V/Δ = 0.64),[17] and are close to those shown by bis-imidazolate complexes. An investigation of the EPR spectrum of [Fe(TMP)(5-MeHIm)₂]ClO₄ in 3:1 DMF−acetonitrile glasses as a function of 5-MeHIm concentration showed that at a ligand−Fe ratio of ~2, the observed *g*-values were 2.89, 2.31, and 1.58, yielding V/λ = 2.07, V/λ = 3.22, and V/Δ = 0.64. As the ligand−Fe ratio was increased, a new rhombic signal began to grow until at a ratio of ~60:1 only the new signal was observed. Its *g*-values were 2.64, 2.30, and 1.80, yielding V/λ = 3.10, Δ/λ = 4.09, and V/Δ = 0.76. Figure 9 illustrates these limiting EPR spectra. These values are much more reasonable for a bis-imidazolate complex and we thus conclude that the middle *g*-value observed for the crystalline sample is skewed by a non-random orientation of the molecules in the EPR sample. The value of Δ/λ observed for the crystalline sample (2.83) is much too small for imidazolate, which is a stronger field ligand than neutral imidazole, for which values

(65) (a) Bois-Poltoratsky, R.; Ehrenberg, A. *Eur. J. Biochem.* **1967**, *2*, 361−365. (b) Passon, P. G.; Reed, D. W.; Hultquist, D. E. *Biochim. Biophys. Acta* **1972**, *275*, 51−61. (c) von Bodman, S. B.; Schuler, M. A.; Jollie, D. R.; Sligar, S. G. *Proc. Natl. Acad. Sci. U.S.A.* **1986**, *83*, 9443−9447. (d) Rivera, M.; Barillas-Mury, C.; Christensen, K. A.; Little, J. W.; Wells, M. A.; Walker, F. A. *Biochemistry* **1992**, *31*, 12233−12240. (e) Guzov, V. M.; Houston, H. L.; Murataliev, M. B.; Walker, F. A.; Feyereisen, R. *J. Biol. Chem.* **1996**, *271*, 26637−26645.

of 3.00–3.32 are common (vide supra). Thus the frozen solution value of $\Delta/\lambda = 4.09$ is much more consistent with the imidazolate formulation. This is an example of the distortion of the EPR spectra of powdered solid samples by non-random orientation of crystallites, and points out the importance of parallel solution measurements.

Using the solution g-values, it is interesting to note that Δ/λ (4.09) for [Fe(TMP)(5-MeHIm)$_2$]ClO$_4$ is close to that typical for iron(III) porphyrinates with the mixed axial ligand combination imidazole/imidazolate ($\Delta/\lambda = 4.44$)[66] and smaller than that with two axial imidazolate ligands, for example, [(K222)][Fe(TPP)(5-MeIm)$_2$] ($\Delta/\lambda = 4.94$).[67] The value of Δ/λ for [Fe(TMP)(5-MeHIm)$_2$]ClO$_4$ is similar to the values reported for several heme proteins at high pH, for example, cytochrome b_5 at pH 11.5 ($\Delta/\lambda = 3.87$, histidine/histidinate form)[68] and the 5-MeIm$^-$ complex of metmyoglobin at pD 10.8 ($\Delta/\lambda = 4.29$ histidine/imidazolate).[69] This suggests that H-bonding between the coordinated 5-MeHIm ligands of *paral*-[Fe(TMP)(5-MeHIm)$_2$]ClO$_4$ and the "solvent" 4(5)-MeHIm molecules within the asymmetric unit indeed imparts partial imidazolate character to at least one axial ligand of each cation.

There are two final considerations that should be drawn from the EPR data. As has been noted, the axial ligand dihedral angles in the two crystalline forms deviate significantly from the ideal values for perpendicular and parallel orientations. Nonetheless, the complexes show limiting type EPR spectra, with the solid-state EPR spectrum of *perp*-[Fe(TMP)(5-MeHIm)$_2$]ClO$_4$ (dihedral angle = 76°) that of a large g_{max} signal while that for *paral*-[Fe(TMP)(5-MeHIm)$_2$]ClO$_4$ (dihedral angle = 30°, two molecules) is rhombic. This leads to the question of where the dividing line in EPR spectral type as a function of the ligand orientation is to be found, and thus what the histidine dihedral angles may be for the membrane-bound cytochromes b of the mitochondrial electron-transport chain and the similar cytochrome b_6 heme centers found in chloroplasts.[70] Structural data for the former are approaching a resolution where it may soon be possible to determine these angles.[71,72] It is unfortunate that the EPR spectral type of the first reported imidazole derivative, [Fe(TPP)(HIm)$_2$]Cl,[58] with its 57° imidazole dihedral angle, was not reported. (To this day it has not been possible to regrow crystals of this particular form.)

The major change in electronic structure that accompanies changes in the axial ligand dihedral angles is the energy difference between the d$_{yz}$ and d$_{xz}$ orbitals, e.g., the Jahn–Teller stabilization energy. A convenient measure of the relative Jahn–Teller stabilization energy, Δ/λ, can be obtained from EPR spectra. Δ/λ for complexes with relative parallel orientations is in the range 2–3.3. For the particular case of *paral*-[Fe(TMP)(5-MeHIm)$_2$]ClO$_4$ in solution, Δ/λ is in the range of 2.1 to 3.1. Although Δ/λ cannot be determined from the powder EPR spectrum of *perp*-[Fe(TMP)(5-MeHIm)$_2$]ClO$_4$, we estimate that $\Delta/\lambda \leq 1$ based on the values found previously for [Fe(TMP)-

(4-NMe$_2$Py)$_2$]$^+$ (0.7–0.9)[15] and [Fe(TPP)(2-MeHIm)$_2$]$^+$ (0.9).[13] A lower limit of Δ/λ for *perp*-[Fe(TMP)(5-MeHIm)$_2$]ClO$_4$ would be ~0.4, given the magnitude of the spitting observed in [Fe(TPP)(CN)$_2$]$^-$ (0.44).[10]

The Jahn–Teller stabilization energy thus depends on the magnitude of the spin–orbit coupling constant, λ. For Fe^{3+} (g),[73] λ is 460 cm^{-1} and is expected to be reduced to between ~300 and 400 cm^{-1} for ferrihemes.[13,74] For *perp*-[Fe(TMP)(5-MeHIm)$_2$]-ClO$_4$, the crystal field stabilization energy can then be estimated at ≤ 0.9–1.2 kcal/mol, while for *paral*-[Fe(TMP)(5-MeHIm)$_2$]-ClO$_4$ the estimated value will be 1.8–3.9 kcal/mol. The electronic stabilization for a relative parallel orientation of the axial ligands is thus less than ~3.0 kcal/mol.

Molecular Mechanics Calculations. Two objectives of this study were to determine how steric interactions affect the relative stabilities of isomers of [Fe(TMP)(5-MeHIm)$_2$]$^+$ (and related species such as [Fe(TPP)(5-MeHIm)$_2$]$^+$) and to understand how conformational changes might affect the coordination geometry of the iron(III) ion in [Fe(TMP)(5-MeHIm)$_2$]$^+$.

The conformational surfaces for [Fe(TMP)(5-MeHIm)$_2$]$^+$ and [Fe(TPP)(5-MeHIm)$_2$]$^+$ shown in Figure 7 differ mainly in the number of maxima and minima. Although both have global minima at ϕ_1, $\phi_2 = 45°$ (S$_4$-ruffled core conformation), the steric energy for [Fe(TMP)(5-MeHIm)$_2$]$^+$ reaches a maximum when the axial ligands have a relative parallel orientation and point at the *meso*-mesityl groups (planar core conformation; ϕ_1, ϕ_2 = 45°, 135°). For [Fe(TPP)(5-MeHIm)$_2$]$^+$, this region clearly corresponds to a local minimum. Since a plot of the change in nonbonded energy with axial ligand orientation (Figure S1) for [Fe(TMP)(5-MeHIm)$_2$]$^+$ also reaches a maximum at this point (ϕ_1, $\phi_2 = 45°$, 135°), nonbonded interactions between the axial 5-MeHIm ligands and the *o*-methyl groups of TMP destabilize a relative parallel orientation for the axial ligands.[75] A relative parallel axial ligand orientation is also destabilized when the ligands eclipse a pair of trans Fe–N$_p$ bonds (e.g., when ϕ_1, ϕ_2 = 0°, 180°).

Interestingly, the conformation observed in the X-ray structure of *perp*-[Fe(TMP)(5-MeHIm)$_2$]$^+$ lies ~0.4 kcal/mol from the global minimum (point **2** in Figure 7). The marked stability of this conformation relative to all other conformational isomers is brought about by S$_4$-ruffling of the porphyrin core (Table 3).[34] Point **1** in Figure 7, in contrast, shows the location of molecule A of the X-ray structure of *paral*-[Fe(TMP)(5-MeHIm)$_2$]ClO$_4$ on the potential surface.[56] This conformation is ~2.6 kcal/mol higher in energy than the global minimum and is located close to the local maximum that has the imidazole planes eclipsed and positioned over a pair of trans Fe–N$_p$ vectors (ϕ_1, ϕ_2 = 0°, 180°). Since the axial 5-MeHIm ligands are close to eclipsing a pair of trans Fe–N$_p$ bonds at point **1**, nonbonded interactions between the imidazole α-hydrogens and the porphyrin nitrogens (Figure S1) account for the higher steric energy of this conformer relative to that of *perp*-[Fe(TMP)(5-MeHIm)$_2$]ClO$_4$.

Varying the axial ligand orientations of [Fe(TMP)(5-MeHIm)$_2$]$^+$, and thus the porphyrin conformation, perturbs the coordination geometry of the metal ion.[76] Figure 8a shows that

(66) Quinn, R.; Nappa, M.; Valentine, J. S. *J. Am. Chem. Soc.* **1982**, *104*, 2588–2595.

(67) Quinn, R.; Strouse, C. E.; Valentine, J. S. *Inorg. Chem.* **1983**, *22*, 3934–3940.

(68) Bois-Poltoratsky, R.; Ehrenberg, A. *Eur. J. Biochem.* **1967**, *2*, 361–365.

(69) Gadsby, P. M. A.; Thomson, A, J. *J. Am. Chem. Soc.* **1990**, *112*, 5003–5011.

(70) Widger, W. R.; Cramer, W. A.; Hermann R. G.; Trebst, A. *Proc. Natl. Acad. Sci. U.S.A.* **1984**, *81*, 674. Babcock, G. T.; Widger, W. R.; Cramer, W. A.; Oertling, W. A.; Metz, J. *Biochemistry* **1985**, *24*, 3638.

(71) Xia, D.; Yu, C.; Kim, H.; Xia, J.; Kachurin, A. M.; Zhang, L.; Yu, L.; Deisenhofer, J. *Science* **1997**, *277*, 60–66.

(72) Iwata, S.; Lee, J. W.; Okada, K.; Lee, J. W.; Iwata, M.; Rasmussen, B.; Link, T. A.; Ramaswamy, S.; Jap, B. K. *Science* **1998**, *281*, 64–71.

(73) Figgis, B. N.; Lewis, J. In *Techniques of Inorganic Chemistry*; Jonassen, H. B., Weissberger, A., Eds.; Wiley Interscience: New York, 1965; Vol. IV, p 159.

(74) Maltempo, M. M. *J. Chem. Phys.* **1974**, *61*, 2540–2547. Levin, P. D.; Brill, A. S. *J. Phys. Chem.* **1988**, *92*, 5103–5110.

(75) Previously we found that nonbonded interactions between the porphyrin mesityl substituents and pyridine ligands in low-spin bis-pyridine derivatives of [Fe(TMP)]$^+$ favor a relative perpendicular axial ligand orientation,[19,35] consistent with the conformational surface for [Fe(TMP)-(5-MeHIm)$_2$]$^+$ shown in Figure 7.

the calculated average $Fe-N_p$ bond length increases from ~1.965 Å for an S_4-ruffled conformation (ϕ_1, $\phi_2 = 45°$) to ~1.985 Å for a planar conformation (ϕ_1, $\phi_2 = 45°$, 135°). This trend is in fact observed experimentally. For example, the mean $Fe-N_p$ bond distance varies from 1.937(12) Å in the strongly S_4-ruffled complex $[Fe(TMP)(1,2-Me_2Im)_2]ClO_4$[34] to 1.987(1) Å in $[Fe(TMP)(1-MeIm)_2]ClO_4$ (planar core conformation).[15]

The difference in the mean calculated bond length for orthogonal pairs of trans $Fe-N_p$ bonds (i.e., those along the *x*- and *y*-directions) also depends on ligand orientation. Figure 8b indicates that this difference, Δ_{xy}, becomes largest when the axial ligands have a relative parallel orientation and nearly eclipse a pair of trans $Fe-N_p$ bonds (e.g., when ϕ_1, $\phi_2 = 18°$, 162°). Unfavorable nonbonded interactions between the axial ligands and eclipsed atoms of the porphyrin core are apparently minimized by slight adjustment of the $Fe-N_p$ bonds. Thus, some asymmetry in metal–porphyrin bonding may be introduced by changes in porphyrin–ligand nonbonded interactions. However, although the X-ray structures of $[Fe(TPP)(HIm)_2]^+$ [16] and $[Fe(TPP)(t-MU)_2]^+$ [37] show such a distortion, the $Fe-N_p$ bonds of the X-ray structures of *paral*-$[Fe(TMP)(5-MeHIm)_2]^+$ do not exhibit an experimentally significant degree of asymmetry.

Finally, Figure 8c shows that the average calculated $Fe-N_{ax}$ bond distance increases from 1.958 Å in the S_4-ruffled conformation of $[Fe(TMP)(5-MeHIm)_2]^+$ (ϕ_1, $\phi_2 = 45°$) to 1.981 Å when the planes of the axial ligands are parallel and eclipse a pair of trans $Fe-N_p$ bonds (ϕ_1, $\phi_2 = 0°$, 180°). These structural changes largely reflect the increase in ligand–porphyrin nonbonded interactions as the ligand planes switch from a staggered arrangement over an S_4-ruffled core to an eclipsed arrangement over a pair of trans $Fe-N_p$ vectors. Although ϕ is not a quantitative predictor of $Fe-N_{ax}$ bond length,[53] experimental evidence for variation of the mean $Fe-N_{ax}$ distance with ligand orientation exists. For example, the X-ray structures of $[Fe(TPP)(HIm)_2]Cl$[16] have mean $Fe-N_{ax}$ bond distances of 1.964-(3) and 1.977(3) Å for axial imidazole orientations of 41° and 6°, respectively.

Ligand Orientation Preferences: Final Comments. Relative parallel orientations are the apparently preferred orientation for most characterized iron(III) porphyrinates having two planar axial ligands, with relative perpendicular orientations observed

only in special circumstances—primarily that of introduced steric effects. However, $[Fe(TMP)(5-MeHIm)_2]ClO_4$ has been obtained in two distinct crystalline forms with different relative ligand orientations. One form, *perp*-$[Fe(TMP)(5-MeHIm)_2]ClO_4$, has a relative perpendicular axial ligand arrangement, a small Mössbauer quadrupole splitting, and a large g_{max} EPR spectrum with a single observable *g*-value. The second form, *paral*-$[Fe(TMP)(5-MeHIm)_2]ClO_4$, has a near-parallel axial ligand orientation, a large Mössbauer quadrupole splitting, and a EPR spectrum with a rhombic **g** tensor. The appearance, in the solid state, of ligand orientations approaching the two limiting forms speaks to a near energetic equivalence of conformational isomers. The energy balance between the two forms is the result of crystal field stabilization effects favoring the parallel form and steric strain effects that favor the perpendicular form. Estimates of the two opposing energetic effects are both less than 3.0 kcal/mol. Indeed, stabilization energy estimates are so close that it is easily seen that the energy balance may shift in favor of either conformation depending on factors such as the degree of ruffling of the porphyrin ligand, the nature of the peripheral substituents on the porphyrin ligand including the size of the ortho substituents of the *meso*-aryl groups, and variations in the actual dihedral angle, $\Delta\phi$, between the axial ligand planes.

Supporting Information Available: Complete crystallographic details, final atomic coordinates, anisotropic thermal parameters, fixed hydrogen atom positions, and fractional coordinates for all non-hydrogen atoms of *paral*-$[Fe(TMP)(5-MeHIm)_2]ClO_4$ and *perp*-$[Fe(TMP)(5-MeHIm)_2]ClO_4$ are given in Tables S1–S11; Table S12 gives a table of hydrogen bond distances observed in the solid-state structure of *paral*-$[Fe(TMP)(5-MeHIm)_2]ClO_4$; Figure S1 is a plot of the change in van der Waals energy (kcal/mol) for $[Fe(TMP)(5-MeHIm)_2]^+$ with axial ligand orientation (PDF). This material is available free of charge via the Internet at http://pubs.acs.org.

JA991551W

---

(76) A noteworthy caveat here is that the calculated changes in the $Fe-N_p$ and $Fe-N_{ax}$ bond lengths do not include contributions from imidazole– and porphyrin–iron(III) π-bonding.[12]